Offshore Surface Evaporation Duct Joint Inversion Algorithm Using Measured Dual-Frequency Sea Clutter

Wenjing Zhou ⓘ, Mingwei Shen ⓘ, Yu Zhang, Di Wu ⓘ, and Daiyin Zhu ⓘ

Abstract—In this article, high-precision joint inversion of evaporative duct based on the dual-frequency radar sea clutter data is analyzed to study the abnormal duct environmental phenomenon that occurs over offshore surfaces. As the information of duct environment retrieved by radars with different frequencies is inconsistent, a joint optimization model with dynamic penalty factor is proposed, which can improve the degree of conformity between the measured clutter power and the modeled clutter power. Then, a parallel crossover quantum particle swarm optimization algorithm is used to jointly invert the objective function, which adaptively processes the inputs involved in the crossover and effectively improves the convergence of the inversion. Compared with the single-frequency model commonly used in engineering, the average relative error of the duct height of the dual-frequency joint optimization model is reduced by 3.13%, and the average relative error of the duct intensity is reduced by 6.34%, verifying the effectiveness of this method.

Index Terms—Dynamic penalty factor, evaporation duct, joint inversion, objective function, radar sea clutter.

I. INTRODUCTION

EVAPORATIVE duct is an electromagnetic environment that frequently occurs in the troposphere above the sea surface [1]. It is formed by the rapid change of atmospheric humidity at a vertical distance due to the evaporation of water vapor from the sea surface. In this space environment, the performance of almost all electronic systems will be affected [2]. The electromagnetic wave bends to the sea surface in the process of propagation, similar to the propagation of a metal waveguide, and the action distance increases, resulting in over-the-horizon propagation. There will also be a certain detection blind area, and the target located in the blind area cannot be accurately detected,

Wenjing Zhou and Mingwei Shen are with the College of Computer and Information Engineering, Hohai University, Nanjing 210024, China (e-mail: 15637357907@163.com; smw_hhu1981@163.com).

Yu Zhang is with the College of Electronic and Electrical Engineering, Henan Normal University, Xinxiang 453007, China (e-mail: hsdzhangyu@126.com).

Di Wu and Daiyin Zhu are with the Key Laboratory of Radar Imagine and Microwave Photonics, Ministry of Education, Nanjing University of Aeronautics and Astronautics, Nanjing 210016, China (e-mail: wudi82@nuaa.edu.cn; zhudy@nuaa.edu.cn).

which greatly affects the detection accuracy [3]. Therefore, real-time high-precision measurement of environmental parameter characteristics and corresponding correction measures play an important role in the performance of electronic systems [4]. At present, the use of radar sea clutter information to retrieve duct parameters is relatively mature in theory and technology. In particular, the Wallops Island experiment in 1998 promoted the research process of radar clutter inversion of duct parameters. Based on it, Rogers et al. [5] introduced an objective function based on the least squares and used an inversion algorithm to solve the duct parameters. The inversion results were in concordance with the actual measurements.

The follow-up research is mainly on the optimization of the objective function and the inversion algorithm. For the objective function, a stable refractive index value is obtained by multiple observations to improve the inversion accuracy. The observed values include radar clutter data obtained from multiple antenna heights, multiple radars, or multiple antenna elevation angles [6]–[8]. However, the above methods all establish multiobjective functions for Pareto solution search, and the contradiction between the subobjective functions makes it difficult to find the solution vector in the constraint set to minimize the N objective functions at the same time. Aiming at the ill-posed relationship between the radar echo data and the refractive index parameters, a global optimization algorithm is used to obtain the approximate solution of the objective function. Matsko and Hackett [9] used a genetic algorithm for inversion; Zhao et al. [10] introduced the Markov chain and used particle filtering to invert the refractive index parameters; in the subsequent research, the genetic algorithm was used to obtain the atmospheric refractive index profile, and the regularization parameter was introduced to improve the profile structure [11]. Other researchers have also introduced alternative algorithms, such as orthogonal artificial bee colony algorithm [12], particle swarm algorithm [13], and Kalman filter algorithm [14]. However, the inversion results of all the above methods are still not accurate or effective enough. In this article, we have, first of all, improved the objective optimization function. According to the different environmental information contained in radar clutter of different frequencies, the dynamic penalty factor is introduced to reduce the measurement noise and increase the clutter-to-noise ratio (CNR), which effectively improves the accuracy of the model inversion. Then, according to the fast convergence characteristics of the quantum particle swarm optimization (QPSO) algorithm [15], adaptive
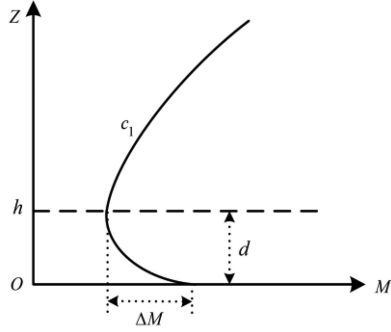
Fig. 1.   Evaporation duct parameter model.

parallel orthogonal crossover and simple crossover factors are introduced into the algorithm, creating an improved algorithm that effectively inverts the objective function.

The rest of this article is organized as follows. Section II introduces the calculation of radio wave propagation power based on the single-frequency model in the evaporative duct environment. Section III proposes a joint optimization model of evaporative duct based on multifrequency sea clutter, adding dynamic penalty factor to the objective function. Section IV proposes an improved algorithm, an adaptive parallel cross-quantum particle swarm optimization (APC-QPSO) algorithm. Section V uses the actual measurement data to verify the content of Sections III and IV. Finally, Section VI concludes this article.

II. SINGLE-FREQUENCY MODEL USING SEA CLUTTER

The offshore tropospheric duct is an abnormal atmospheric refractive index structure. When researching the inversion problem, the profile model can be established according to the refractive index characteristics of the duct environment. An exponential model is often used, which is simple to calculate and has good consistency between the described profile and the actual measurement [16]. The schematic diagram of the model is shown in Fig. 1, and the formula is as follows:

$$M(z) = M(z_0) + 0.125z - 0.125d \times \ln \frac{z + z_0}{z_0} \quad (1)$$

$$\Delta M = |M(d) - M(z_0)|. \quad (2)$$

The evaporation duct height d and the duct intensity ΔM are taken as the inversion parameters $\boldsymbol{m}$. The maximum value of the vertical height z is 500 m. $M(z_0)$ is the modified refractive index value at the sea surface, and its value is 339; z_0 takes the initial value of 0.1 m.

In the tropospheric evaporative duct environment, the antenna elevation angle is small and the radio wave propagation problem can be described by the standard parabolic equation [17]

$$\frac{\partial^2 u}{\partial^2 z}(x, z) + 2ik \frac{\partial u}{\partial x}(x, z) + k^2(n^2(x, z) - 1)u(x, z) = 0 \quad (3)$$

where k is the wavenumber in vacuum, x is the horizontal propagation distance, n is the refractive index, and u is the field distribution.

The attenuation factor A of radio wave propagation is expressed as

$$A = \sqrt{x} |u(x, z)|. \quad (4)$$

The wave propagation loss is

$$L = L_{fs} + A \quad (5)$$

where L_{fs} is the free propagation loss.

The radar sea clutter power P_c can be obtained from the radar equation

$$P_c(\boldsymbol{m}, x) = -2L(\boldsymbol{m}, x) + 10\log_{10} x + \sigma^0 + C \quad (6)$$

where x is the distance between the radar and the detection target; σ^0 is the scattering coefficient, which is obtained by the radar sea clutter model; and C is a constant related to the marine environment and radar parameters.

III. JOINT OPTIMIZATION MODEL BASED ON THE DUAL-FREQUENCY SEA CLUTTER

The process of using radar sea clutter to invert the profile parameters of the evaporative duct is actually to obtain the profile parameter information when the simulated power data and the measured power data have the highest agreement [18]. By establishing the objective function between the power database and the measured power, using the optimization algorithm to solve it, the profile parameter information corresponding to the minimum objective function is obtained.

Studies have shown that the clutter power data obtained by different radar frequencies have different structures and changes, which affect the inversion results of profile parameters [8], [19]. Therefore, the impact on the power bank needs to be considered when using dual-frequency radar data. Through modeling and simulation, a clutter power database containing two-frequency sublibraries is obtained. Assuming that the radar frequencies are f_1 and f_2, the clutter power sublibrary can be expressed as

$$P_i^{cal}(\boldsymbol{m}, x, f_i) = -2L(\boldsymbol{m}, x, f_i)$$
$$+ 10\log_{10} x + \sigma^0 + C, (i = 1, 2) \quad (7)$$

where P_i^{cal} represents the modeling value of radar frequency f_i. The discrete clutter power data received by the radar with frequency f_1 are P_1^{obs}, and the discrete clutter power data received by the radar with frequency f_2 are P_2^{obs}; then, the subobjective function between the measured discrete clutter power data and the clutter power library is expressed as follows:

$$\phi_i(\boldsymbol{m}) = \sum_{j=0}^{N-1} \left[P_i^{obs}(x_j) - P_i^{cal}(\boldsymbol{m}, x_j) \right]^2, (i = 1, 2) \quad (8)$$

where N is the number of discrete data, and x_0 is the initial receiving distance of the inversion radar sea clutter. Since the power data near the coast are easily interfered by environmental noise, the value of x_0 is 10 km; x_{N-1} is the farthest receiving distance measured.

In the actual inversion, the echo signal received by the radar is not only accompanied by clutter information but also superimposed with measurement noise. The clutter power calculated

by the forward model is ideal and noise-free data, and the clutter power measured by the radar will be interfered by the noise of the receiver itself and environmental noise, so the accuracy of the inversion results will inevitably be affected. Based on the least squares estimation, this article proposes an objective function with a dynamic penalty factor. According to the dual-band radar data information, the multiobjective optimization is converted into single-objective optimization by using the penalty factor, and the optimal compromise value between the subobjective functions is obtained, which reduces the interference of measurement noise and improves the model inversion accuracy.

According to the radar equation, the clutter power has the fourth power attenuation relationship with the distance, and the overall trend of the clutter power gradually decreases with the increase of the distance. Therefore, the CNR is relatively large at the distance x_0, which can be used to measure the compromise value between the subobjective functions [20]. Here, the penalty factor can be expressed as a function of the duct parameter value $\boldsymbol{m}$ and the power value at the initial acceptance distance x_0

$$\alpha_0 = \frac{\phi_1(\boldsymbol{m}, x_0)}{\phi_2(\boldsymbol{m}, x_0)} = \frac{\left[P_1^{obs}(x_0) - P_1^{cal}(\boldsymbol{m}, x_0)\right]^2}{\left[P_2^{obs}(x_0) - P_2^{cal}(\boldsymbol{m}, x_0)\right]^2}. \quad (9)$$

It can be seen from the above formula that the penalty factor changes nonlinearly and adaptively with the clutter power sublibrary and the clutter power measurement value at x_0 during the inversion process. The clutter power sublibrary has the corresponding penalty factor for different evaporative duct environments (different duct parameter values), thereby obtaining the optimal compromise value between subobjective functions established based on the dual-frequency data. By introducing the penalty factor, the optimized objective function is obtained as follows:

$$\min F(\boldsymbol{m}) = \sum_{j=0}^{N-1} \left[P_1^{obs}(x_j) - P_1^{cal}(\boldsymbol{m}, x_j)\right]^2$$

$$+ \alpha_0 \sum_{j=0}^{N-1} \left[P_2^{obs}(x_j) - P_2^{cal}(\boldsymbol{m}, x_j)\right]^2. \quad (10)$$

When the number of frequencies is single, it is the basic single-frequency objective function solution in the inversion problem.

IV. ADAPTIVE PARALLEL CROSS-QUANTUM PARTICLE SWARM OPTIMIZATION

The QPSO algorithm [21] introduces the compressive expansion factor and the average particle optimal position according to the motion law of the particles in the quantum space and uses the wave function to represent the position information and the Monte Carlo method to solve the particle position. Assuming that the particle is l and its position is y, the update equation is as follows:

$$l_{i,j}(t) = \varepsilon p\text{best}_{i,j}(t) + (1 - \varepsilon)g\text{best}_j(t) \quad (11)$$

$$m\text{best}_j(t) = \frac{1}{N}\sum_{i=1}^{N} p\text{best}_{i,j}(t) \quad (12)$$
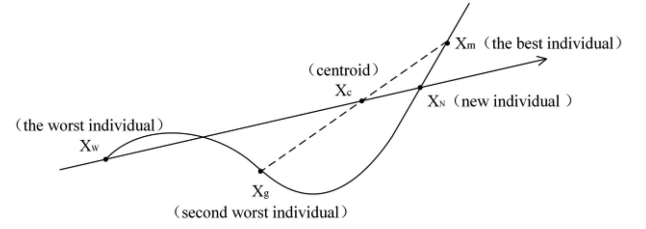

Fig. 2. Simplex cross schematic.

$$y_{i,j}(t+1) = l_{i,j}(t) \pm v|m\text{best}_j - y_{i,j}(t)| \cdot \ln\left(\frac{1}{u}\right) \quad (13)$$

where $l_{i,j}(t)$ is the random position of each particle between the individual optimal position $p$best and the global optimal position $g$best; $m$best is the average of the optimal positions of all particles introduced in the QPSO algorithm; ε and u are uniformly distributed random numbers in the interval $(0,1)$, and φ is the expansion–compression factor; formula (13) is the iterative equation of particle position.

However, the QPSO algorithm loses the diversity of population when solving complex multivalue functions, making it difficult to achieve the intended precision. Therefore, the orthogonal crossover operator and simplex crossover operator are introduced in this article so that a particle has multiple uncertain states and the position is updated. The obtained multiple particles form the parent group after which the child individual is obtained through the crossover operation so as to achieve global optimization and maintain the diversity of the population.

The improved algorithm deceptively divides the groups into two categories according to the fitness value of each iteration, an excellent group (with relatively good fitness value) and an inferior group (with relatively poor fitness value). The orthogonal crossover operator is introduced in the excellent group, and the simplex crossover operator is introduced in the inferior group. The parallel use of the two crossover operators not only greatly improves the population diversity of the QPSO algorithm but also reduces the computational burden brought by the introduction of crossover operators and accelerates the convergence speed.

The particles in the optimal group are orthogonally crossed with an adaptive crossover probability to achieve the dual goals of maintaining diversity and convergence. The expression is as follows:

$$\varphi = \begin{cases} k_1 - \frac{(f - f_{\text{avg}})}{f_{\max} - f_{\text{avg}}}, & f \leq f_{\text{avg}} \\ k_2, & f > f_{\text{avg}} \end{cases} \quad (14)$$

where k_1 is 0.9; k_2 is 0.6; f_{avg} is the average fitness value; and f is the current fitness value.

Simultaneously, the simplex crossover operator is used to search the inferior population. The simplex crossover schematic is shown in Fig. 2. The worst individual X_w is selected as the initial point of the simplex search; the optimal individual X_m is used as the target point; the worst individual X and other random individuals are used to estimate the directional gradient. The direction is from X_w to the centroid X_c of the other individuals except the worst point. After four basic operations—reflection

point expansion, reflection point compression, worst point compression, and overall shrinkage, individuals with good fitness values are searched to replace the original worst ones. This crossover operator enables multiple individuals to generate new individuals, and while maintaining the diversity of the population, it limits the excessive use of search and accelerates the convergence speed.

The simplex crossover operator is shown in the following formula, and each crossover can obtain three different subindividuals:

$$X_m = \begin{cases} X_c - \alpha \left(X_c - X_w \right) \\ X_c + \alpha \left(X_c - X_w \right) \\ \left(2X_c - X_w \right) - \alpha \left(X_c - X_w \right) \end{cases} \quad 0 < \alpha < 1. \quad (15)$$

The inferior population L are divided into multiple local groups, each of which contains n individuals, and a local individual is randomly selected as the starting point of simple crossover to obtain a subgroup with $3n$ individuals. Then, by performing $[L/n]$ simple iterations ([] is the rounding symbol), a subpopulation P_{g2} containing $[L/n] \times 3n$ individuals can finally be generated.

After parallel crossover, the group $(P_{g1}+P_{g2})$ is obtained, and the fitness of the subgroup is evaluated to obtain the individual optimal position and the global optimal position. Then, proceed to the next iteration.

Based on the introduction of the APC-QPSO algorithm in Section III, combined with the background requirement of obtaining the minimum value of the established objective function for the solution of the evaporation duct profile parameters, the APC-QPSO algorithm flow for minimizing the function is as follows:

Begin
  Initialize algorithm parameters (iteration number G, population size N, initial particle swarm P_0, initial particle position y);
  Repeat 1
    Get the average optimal position $m$best of particles;
    Repeat 2
    Use formulae (11)–(13) to update the particle position; obtain particle group P_1 through particle collapse; divide group P_1 into superior group and inferior group;
  If Excellent group
    Use formula (14) to perform orthogonal crossover operations to obtain the population P_{g1};
  End if
  If Inferior group
    Use (15) to perform the simplex crossover operation to obtain group P_{g2};
  End if
  Obtain the group $(P_{g1} + P_{g2})$, and update the optimal individual and fitness value;
  Until 2 Until the loop N times, end;
  Save the current optimal solution and optimal position;
  Until 1 Until the loop G times, end;
End.

TABLE I
RADAR AND ENVIRONMENTAL PARAMETERS

	Parameters/Units	Numerical value
	Frequency/Ghz	10,12
	Transmit power/dBm	90
	Beamwidth/°	0.5
Radar parameters	Antenna Type and Polarization	Gaussian，HH
	Antenna gain/dB	54
	Antenna elevation angle/°	0.1
	Antenna height/m	8
Two experimental environments: Lianyungang, Rizhao	Water vapor temperature/°	20.4 ; 21.7
	Relative humidity	60.1% ; 50.7%
	Air pressure/hPa	1023.3 ; 1012.9
	Wind speed/m/s	0.5 ; 2.2
	Wind direction	159 ; 92.9

V. EXPERIMENTAL ANALYSIS

A. Performance Analysis of the APC-QPSO Algorithm

In order to prove the feasibility and effectiveness of the objective function with dynamic penalty factor and the improved algorithm APC-QPSO proposed in this article, the experimental data measured on the coast of Lianyungang and Rizhao in October 2020 were used for verification. The environmental database from Advanced Refractive Effects Prediction System (AREPS) evaporative duct statistical information divides the earth's latitude and longitude into Marston's grid, among which Lianyungang and Rizhao belong to the MS132 sea area [16]. According to the radar parameter table applicable to the evaporative duct inversion in different sea areas and months, a radar with the antenna height of 8 m and the frequency of 10 and 12 GHz was selected to obtain the measured radar sea clutter power. The specific radar parameters and environmental parameters are shown in Table I. The microwave refractometer offers high accuracy and real-time performance and is suitable for the measurement of evaporation duct profiles within 50 m in height. Therefore, this article uses a refractometer carried by a liftable boom to measure the height and intensity of the evaporation duct synchronously.

In the experiment, two shore-based radars with frequencies of 10 and 12 GHz were used to detect targets at a distance of 210 km under the same time and space conditions, and the measured sea clutter power data with sea surface environmental information are acquired. By discretizing the measured data, (the value interval is 2 km), the measured power with 100 data values is obtained. According to the theoretical model, the value of the evaporation duct height d is in the range [5,40] m, and its step value is 0.01; the horizontal distance range is 200, and 100 discrete data at equal intervals are used for calculation. The clutter power data corresponding to all duct profiles are obtained to form an $n \times s$-dimensional power data sublibrary. It should be noted that the radar frequency is different, and the corresponding clutter power sublibrary is also inconsistent.

In this article, adaptive compression factor particle swarm optimization (APSO) [22], particle swarm optimization with cross factor (CPSO) [23], and QPSO and the improved algorithm

TABLE II
ALGORITHM PARAMETER SETTING TABLE

Algorithm	Different parameter values	Initial population size	Inversion algebra	Number of runs
APSO	c1=1.2; c2=1.5; ω=0.8	50	120	10
CPSO	c1=1.2; c2=1.5; ω=0.8	50	120	10
QPSO	β=0.5	50	120	10
apc-QPSO	β=0.5; Q=4; N=2	50	120	10

APC-QPSO are used to compare the single-frequency objective function and dual-frequency objective function established by two sets of the measured data and clutter power library, and analyze the convergence of the algorithm to prove the effectiveness of the improved algorithm. The preparameter settings of the algorithm are shown in Table II. $c1$ and $c2$ are the learning factors; ω is the inertia weight; β is the compression–expansion factor; N represents the number of orthogonal factors, and Q represents the factor level. The operating system is windows 10 (64-bit), the processor is Intel(R) Core i5-11400F, the running memory is 16 GB, and the compiler is MATLAB2019a. In order to avoid the randomness of some parameters in the initial stage and errors caused by other uncertain factors, the experimental results are the average values obtained from ten runs.

Using the data collected in Lianyungang (Experiment 1), the fitness values of the single-frequency objective function and the dual-frequency objective function under the inversion of the four algorithms are obtained with a maximum number of function evaluations of 6000, as shown in Fig. 3. Comparing the performance of each algorithm under the conditions of Experiment 1, Fig. 3(a)–(c) shows the minimum solution results of frequencies 10 GHz, 12 GHz, and 10 GHz/12 GHz, respectively. From this, we can see that the APC-QPSO algorithm has better optimization results in both the single-frequency objective function and the multifrequency objective function. Compared with APSO and CPSO algorithms, QPSO has the fastest convergence under both single-frequency and dual-frequency conditions and the minimum value can be found with the least number of function evaluations; however, the optimization effect of the QPSO algorithm is worse than the other algorithms, and it is easy to fall into the local optimum. It is difficult to find the global minimum value of the objective function in the 6000 evaluation times, and the calculation results for the three groups of frequency data are relatively poor. After the APC-QPSO algorithm adds a parallel crossover operator to the QPSO algorithm and performs adaptive processing, the algorithm's optimization ability is significantly enhanced. Under the condition that the maximum number of evaluations of the function is 6000, it can be seen from the figure that the overall optimization value of APC-QPSO is smaller than that of QPSO and APSO. Under the conditions of 10 GHz and dual frequency, APC-QPSO can obtain the same objective function value as the CPSO algorithm; under the condition of 12 GHz, it is smaller than the optimal value of CPSO. As for the convergence of the algorithm, the minimum value of
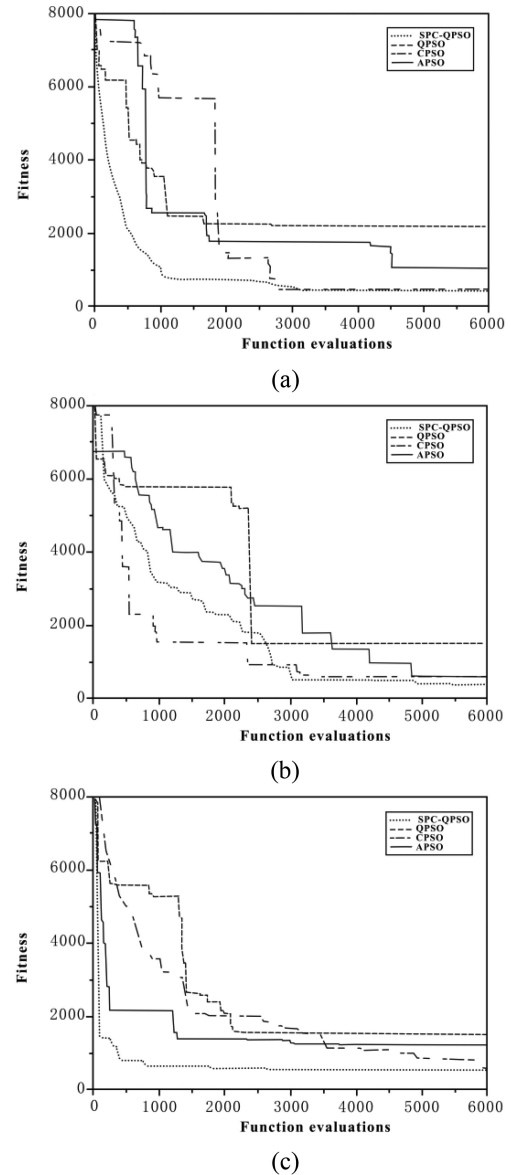

(a)

(b)

(c)

Fig. 3. Iterative optimization diagram of Case1 objective function.

APC-QPSO can be obtained at about 3000 evaluation times, which is much faster than the convergence speed of APSO and CPSO.

The same inversion and data analysis as in Experiment 1 were performed on the data collected in Rizhao (Experiment 2), as shown in Fig. 4. We found out that given the maximum number of evaluations, when the frequency is 12 GHz, the final result of the CPSO algorithm is smaller than the objective function value obtained by APC-QPSO, but in other cases, the calculation results of the two algorithms are equivalent, and both are smaller than APSO and QPSO. Under the dual-frequency condition, the convergence of APC-QPSO and the optimization characteristics under the maximum number of evaluations are excellent. While ensuring the inversion accuracy, the convergence of the algorithm is improved, indicating that the improved algorithm proposed in this article is effective and efficient.
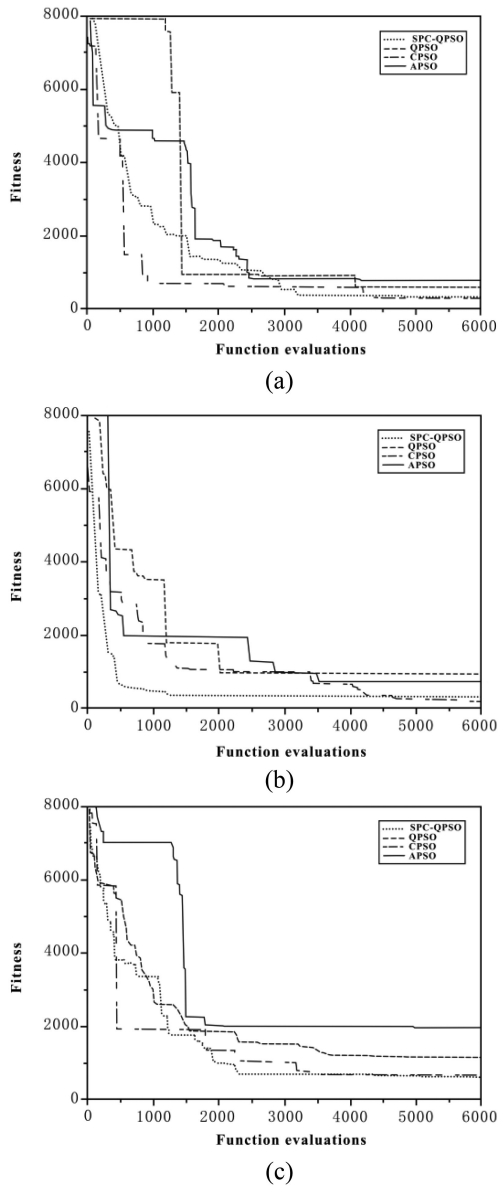
Fig. 4. Iterative optimization diagram of Case2 objective function.

TABLE III
PROFILE PARAMETER RESULTS OF EXPERIMENT 1

	Truth value	10 Ghz	12 Ghz	(10 Ghz\12 Ghz)
d	8.96 m	9.43 m	8.71 m	8.89 m
ΔM	7.81	6.89	6.28	7.33

TABLE IV
PROFILE PARAMETER RESULTS OF EXPERIMENT 2

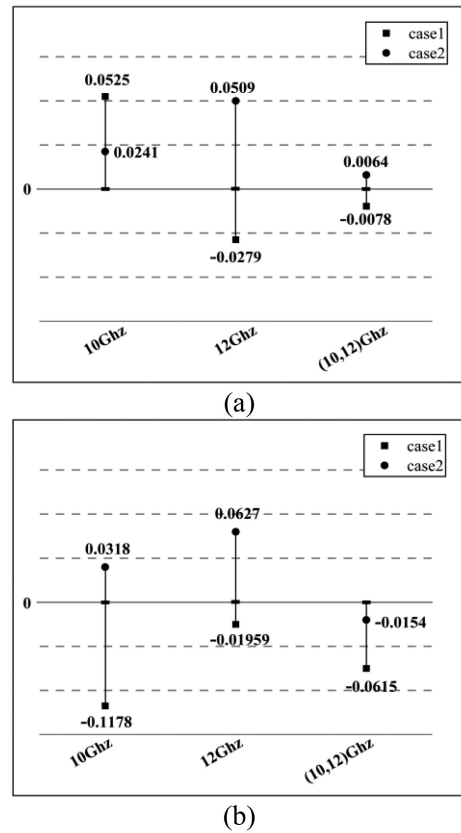|	Truth value	10 Ghz	12 Ghz	(10 Ghz\12 Ghz)
d	14.13 m	14.47 m	14.85 m	14.22 m
ΔM	11.01	11.36	11.70	10.84

Fig. 5. Relative error comparison chart is [(a) relative error comparison of duct height and (b) relative error comparison of duct intensity)].

B. Performance Analysis of the Joint Inversion Method

The experimental data measured by the microwave refractometer and the profile parameter results obtained by the joint inversion model based on the dual-frequency data proposed in this article are compared and analyzed to judge whether the improved inversion model in this article is feasible and effective. In experiment 1, when the observation height was 5.5 m, the measured evaporation duct height was 8.96 m, and the duct intensity was 7.81; in experiment 2, when the observation height was 5.5 m, the measured evaporation duct height was 14.13 m, and the duct intensity was 11.01. The APC-QPSO algorithm was used to perform optimization model inversion for the data with frequencies of 10 GHz, 12 GHz, and the combination of two frequencies, respectively. The results obtained are shown in Tables III and IV.

The relative error value between the measured data and the simulated data is calculated, and the improvement effect of the model is measured by inverting the relative error values of the evaporation duct height and duct intensity. As shown in Fig. 5, (a) represents the relative error comparison of the height of the evaporation duct, and (b) represents the relative error comparison of the intensity of the evaporation duct. In experiment 1, the duct intensity obtained from 10 GHz data is closer to the measured intensity, and the duct height obtained from 12 GHz data is closer to the measured height. After dual-frequency fusion processing, the obtained d and ΔM are better than the single-frequency processing results. In experiment 2, the 10 GHz data are better than the 12 GHz data for both the height of the evaporation
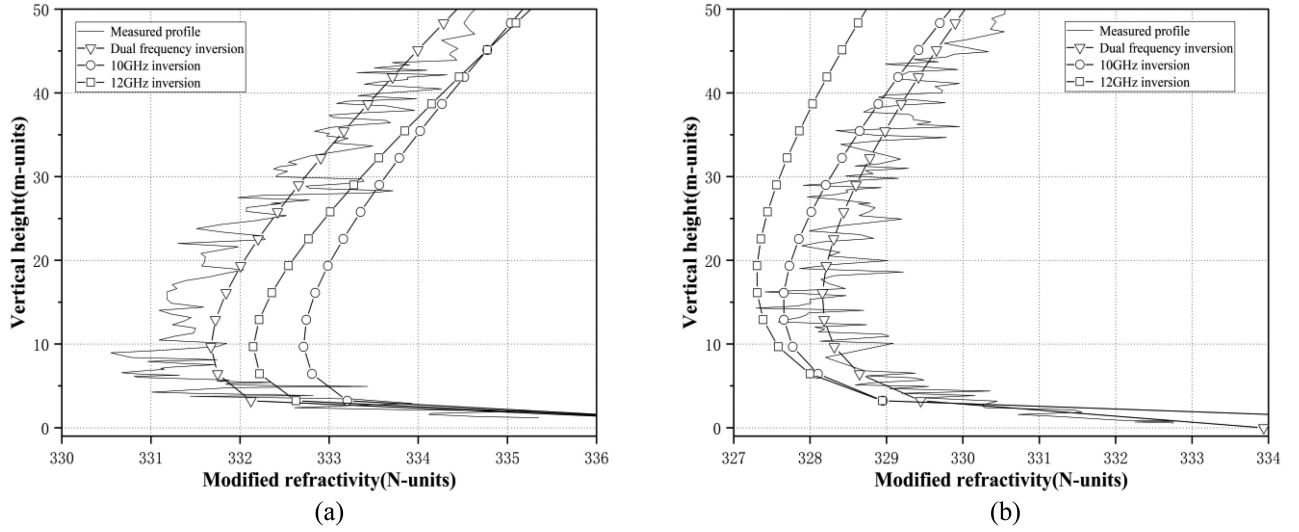
Fig. 6.   Comparison of measured profile and inversion profile. (a) Case 1. (b) Case 2.
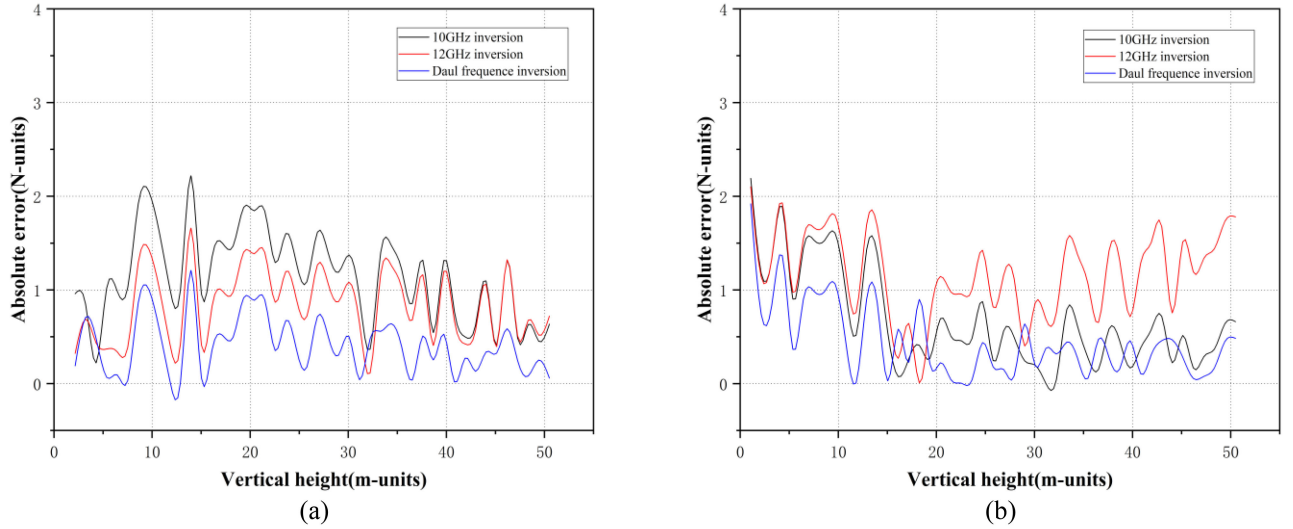

Fig. 7.   Fitting error of the inversion profile. (a) Case 1. (b) Case 2.

duct and the duct intensity, indicating that the 10 GHz data are less disturbed by noise in this environment, and the proportion is larger in the dual-frequency fusion processing. Comparing the results of the single-frequency data with the results after the fusion of the two-frequency data, it can be found that the evaporation duct height and the duct intensity obtained from the dual-frequency data are closer to the real values as compared to the two single-frequency results. The average relative error is given by the expression

$$\varepsilon = \left(\frac{x_1 - \mu_1}{\mu_1} + \frac{x_2 - \mu_2}{\mu_2} \right) /2 \times 100\% \qquad (16)$$

where x represents the real value of the duct parameters, and μ represents the inversion value of the duct parameters. The average relative error of the duct height for the two datasets was reduced by 3.13%, and the average relative error of the

duct intensity was reduced by 6.34%. Therefore, the optimized model of the dual-frequency fusion can more accurately invert the parameter information of the evaporation duct profile than the single-frequency model.

By bringing the obtained inversion parameters into the evaporation duct parameter model, the inversion profile can be obtained. The measured profile, as shown in Fig. 6, is the fitting curve obtained by the microwave refractometer measurement, which is a direct measurement method, suitable for point measurement. Using the measurement profile parameters measured by the instrument, the error between the inversion curves calculated based on the single-frequency and dual-frequency radar measurement echo power can be compared, which can prove the effectiveness of the optimization method described in this article. Fig. 6(a) and (b) shows the modified refractive index–height variation diagrams of the two sets of measurement profiles and

inversion profiles, respectively. It should be noted that, for duct propagation, the relative shape of the refractive index profile is important. In case 1 of Fig. 6(a), it can be clearly seen that the overall refractive index distribution of the dual-frequency inversion is better than that of the two single-frequency inversions. In particular, it optimizes the profile shape with height of more than 27 m, and the duct strength is also very close to the measured value. That is because, in an inversion problem, measurement data with high agreement can give stable and less biased estimates. If the 10 GHz inversion is used as the base measure, the 12 GHz inversion can be viewed as a penalty for having an optimization effect on the solution. The fitting error of inversion profile and measurement profile of case 1 is shown in Fig. 7(a). It can be seen that the overall error value of the dual-frequency inversion is smaller than that of the two single-frequency inversions.

In case 2 of Fig. 6(b), the profile shape of 10 GHz inversion is better than that of 12 GHz inversion, and it can basically get the shape close to the measured profile, but the profile obtained by the dual-frequency combination is the best among the three. And from the profile error in Fig. 7(b), it can be seen that the dual-frequency inversion reduces the error below 15 m and has almost the same error as the single-frequency 10 GHz for the profile with larger height. The above two experimental results show that the dual-frequency inversion profile can basically describe the trend of the measured profile, while the inversion profile of the single-frequency data, whether it is 10 or 12 GHz, is greatly affected by noise; the results are not ideal, and the overall error is large. Through the analysis of the above experimental results, it can be proved that the objective function with dynamic penalty factor proposed in this article and the improved inversion algorithm APC-QPSO algorithm are effective.

VI. Conclusion

In this article, a high-precision joint inversion method for evaporative duct based on the dual-frequency radar sea clutter data is proposed. Using dual-frequency sea clutter data collected in Lianyungang and Rizhao and introducing dynamic penalty factor, a joint optimization model of evaporation duct is established; and the APC-QPSO algorithm is used for efficient inversion of the optimized model. The experimental results show that the inversion accuracy of the proposed algorithm is 3.13% higher than that of the conventional single-frequency model duct height inversion, and the inversion accuracy of the duct intensity is improved by 6.34%, allowing it to more accurately estimate the environmental parameters of the evaporation duct, while the estimated profile is basically consistent with the measured profile.

References

[1] C. Yardim, P. Gerstoft, and W. S. Hodgkiss, "Sensitivity analysis and performance estimation of refractivity from clutter techniques," *Radio Sci.*, vol. 44, no. 1, Feb. 2009, Art. no. RS1008, doi: 10.1029/2008RS003897.

[2] K. Franklin, Q. Wang, D. P. Alappattu, B. Burkholder, C. Yardim, and D. Khelif, "Sensitivity of near-shore electromagnetic propagation to the spatial variability of evaporative duct properties," in *Proc. IEEE Int. Symp. Antennas Propag./USNC/URSI Nat. Radio Sci. Meeting*, 2018, pp. 883–884.

[3] P. Huang, Z. Zou, X.-G. Xia, X. Liu, and G. Liao, "A statistical model based on modified generalized-K distribution for sea clutter," *IEEE Geosci. Remote Sens. Lett.*, vol. 19, no. 99, Jul. 2022, Art. no. 8015805, doi: 10.1109/LGRS.2021.3093975.

[4] P. Huang, Z. Zou, X.-G. Xia, X. Liu, G. Liao, and Z. Xin, "Multichannel sea clutter modeling for spaceborne early warning radar and clutter suppression performance analysis," *IEEE Trans. Geosci. Remote Sens.*, vol. 59, no. 10, pp. 8349–8366, Oct. 2021, doi: 10.1109/TGRS.2020.3039495.

[5] L. T. Rogers, C. P. Hattan, and J. K. Stapleton, "Estimating evaporation duct heights from radar sea echo," *Radio Sci.*, vol. 35, no. 4, pp. 955–966, Jul./Aug. 2000, doi: 10.1029/1999RS002275.

[6] X. Zhao, D. Wang, and S. Huang, "Atmospheric duct estimation from multi-source radar sea clutter returns: Theoretical framework and preliminary numerical results," *Chin. Sci. Bull.*, vol. 59, no. 34, pp. 4899–4906, Dec. 2014, doi: 10.1007/s11434-014-0428-x.

[7] J.-P. Zhang, Z.-S. Wu, Y.-S. Zhang, and B. Wang, "Evaporation duct retrieval using changes in radar sea clutter power versus receiving height," *Prog. Electromagn. Res.*, vol. 126, pp. 555–571, Jan. 2012, doi: 10.2528/pier11121307.

[8] Q. Liao et al., "A comparative study on evolutionary multi-objective optimization algorithms estimating surface duct," *Sensors*, vol. 18, no. 12, Dec. 2018, Art. no. 4428, doi: 10.3390/s18124428.

[9] I. J. Matsko and E. E. Hackett, "Impact of radar data sampling on the accuracy of atmospheric refractivity inversions over marine surfaces," *Radio Sci.*, vol. 54, no. 7, pp. 704–714, Jul. 2019, doi: 10.1029/2018RS006757.

[10] X. F. Zhao, S. X. Huang, and D. X. Wang, "Using particle filter to track horizontal variations of atmospheric duct structure from radar sea clutter," *Atmos. Meas. Techn.*, vol. 5, no. 11, pp. 2859–2866, Nov. 2012, doi: 10.5194/amt-5-2859-2012.

[11] X. Zhao and S. Huang, "Atmospheric duct estimation using radar sea clutter returns by the adjoint method with regularization technique," *J. Atmos. Ocean. Technol.*, vol. 31, no. 6, pp. 1250–1262, Jun. 2014, doi: 10.1175/jtech-d-13-00025.1.

[12] C. Yang and L. Guo, "Inferring the atmospheric duct from radar sea clutter using the improved artificial bee colony algorithm," *Int. J. Microw. Wireless Technol.*, vol. 10, no. 4, pp. 437–445, May 2018, doi: 10.1017/s1759078718000247.

[13] Y. Zhang, W. J. Zhou, X. X. Wang, and M. H. Han, "An improved particle swarm optimization algorithm for inversion of evaporation ducts," *Electron. Opt. Cont.*, vol. 28, no. 11, pp. 1–5, Nov. 2021.

[14] Z. Sheng, "Tracking refractivity from radar clutter using extended Kalman filter and unscented Kalman filter," *Acta Physica Sinica- Chin. Ed.*, vol. 60, no. 11, pp. 820–826, Nov. 2011.

[15] S. L. Ho, S. Yang, G. Ni, and J. Huang, "A quantum-based particle swarm optimization algorithm applied to inverse problems," *IEEE Trans. Magn.*, vol. 49, no. 5, pp. 2069–2072, May 2013, doi: 10.1109/TMAG.2013.2237760.

[16] A. Karimian, C. Yardim, P. Gerstoft, W. S. Hodgkiss, and A. E. Barrios, "Refractivity estimation from sea clutter: An invited review," *Radio Sci.*, vol. 46, no. 6, pp. 1–16, Dec. 2011, doi: 10.1029/2011rs004818.

[17] V. A. Permyakov, M. S. Mikhailov, and E. S. Malevich, "Analysis of propagation of electromagnetic waves in difficult conditions by the parabolic equation method," *IEEE Trans. Antennas Propag.*, vol. 67, no. 4, pp. 2167–2175, Apr. 2019, doi: 10.1109/TAP.2019.2905674.

[18] J. Pozderac, J. Johnson, and C. Yardim, "X-band beacon-receiver array evaporation duct height estimation," in *Proc. IEEE Int. Symp. Antennas Propag. USNC/URSI Nat. Radio Sci. Meeting*, 2015, pp. 916–917, doi: 10.1109/APS.2015.7304845.

[19] R. Hu, Z. Wu, and J. Zhang, "Analysis for best radar parameter in inversion of evaporation duct above China sea areas," *Chin. J. Radio Sci.*, vol. 30, no. 4, pp. 653–660, Aug. 2015, doi: 10.13443/j.cjors.2014080501.

[20] Z.-H. Zhang, Z. Sheng, and H.-Q. Shi, "Parameter estimation of atmospheric refractivity from radar clutter using the particle swarm optimization via Lévy flight," *J. Appl. Remote Sens.*, vol. 9, no. 1, Oct. 2015, Art. no. 095998, doi: 10.1117/1.JRS.9.095998.

[21] O. U. Rehman, S. U. Rehman, S. Tu, S. Khan, M. Waqas, and S. Yang, "A quantum particle swarm optimization method with fitness selection methodology for electromagnetic inverse problems," *IEEE Access*, vol. 6, pp. 63155–63163, 2018, doi: 10.1109/ACCESS.2018.2873670.

[22] W. Zhang, Y. Gao, and C. Zhang, "The enhanced vector of convergence for particle swarm optimization based on constrict factor," in *Proc. IEEE Congr. Evol. Comput.*, 2014, pp. 1337–1342, doi: 10.1109/CEC.2014.6900392.

[23] S. Kong and S. Liu, "Research on missile route planning based on improved particle swarm optimization algorithm," *Meas. Control Technol.*, vol. 36, no. 11, pp. 66–69, 2017.

Wenjing Zhou received the B.S. degree in electronics and information engineering and and M.E. degree in physical electronics from Henan Normal University, Xinxiang, China, in 2021. She is currently working toward the Ph.D. degree in information and communication engineering with Hohai University, Nanjing, China.

Mingwei Shen received the B.S. and Ph.D. degrees in electronic engineering from the Nanjing University of Aeronautics and Astronautics(NUAA), Nanjing, China, in 2003 and 2008, respectively.

He is currently a Professor with the College of Computer and Information Science, Hohai University, Nanjing. His research interests include radar signal processing and adaptive array signal processing.

Yu Zhang received the B.S. degree in electromagnetic field and microwave technology from Xidian University, Xian, China, in 1986.

He is currently a Professor with the College of Electronics and Electrical Engineering, Henan Normal University, Xinxiang, China. His research interests include electromagnetic field and microwave technology.

Di Wu received the B.S. and Ph.D. degrees in electronic engineering from the Nanjing University of Aeronautics and Astronautics (NUAA), Nanjing, China, in 2005 and 2011, respectively.

He is currently a Professor with the College of Electronic Information Engineering, NUAA. His research interests include radar signal processing and high-resolution radar imaging.

Daiyin Zhu received the B.S. degree in electronic engineering from Southeast University, Nanjing, China, in 1996, and the M.S. and Ph.D. degree in electronic engineering from the Nanjing University of Aeronautics and Astronautics (NUAA), Nanjing, in 1998 and 2002, respectively.

He is currently a Professor with the College of Electronic Information Engineering, NUAA. His research interests include radar signal processing and high-resolution radar imaging.